



Dihydroartemisinin increases gemcitabine therapeutic efficacy in ovarian cancer by inducing reactive oxygen species

Shengcai Yang^{1,2} | Dawei Zhang² | Na Shen² | Guanyi Wang² | Zhaohui Tang² | Xuesi Chen^{1,2}

¹College of Chemistry, Jilin University, Changchun, China

²Key Laboratory of Polymer Ecomaterials, Changchun Institute of Applied Chemistry, Chinese Academy of Sciences, Changchun, China

Correspondence

Zhaohui Tang, PhD, Key Laboratory of Polymer Ecomaterials, Changchun Institute of Applied Chemistry, Chinese Academy of Sciences, 5625 Renmin Street, Changchun 130022, China.
Email: ztang@ciac.ac.cn

Funding information

Science and Technology Service Network Initiative, Grant/Award Number: KFJ-SW-STS-166; Ministry of Science and Technology of China, Grant/Award Numbers: 2017zx09101005-012, 2016YFC1100701; Chinese Academy of Sciences Youth Innovation Promotion Association; National Natural Science Foundation of China, Grant/Award Numbers: 51528303, 51390484, 51673189, 51503202, 51520105004

Abstract

Ovarian cancer is the major cause of death in women gynecological malignancy and gemcitabine (GEM) is commonly used in related chemotherapy. However, more than 90% GEM is catalyzed into an inactive metabolite 2'-deoxy-2',2'-difluorouridine by stromal and cellular cytidine deaminase (CDA). Dihydroartemisinin (DHA), which possesses an intramolecular endoperoxide bridge, could be activated by heme or ferrous iron to produce reactive oxygen species (ROS). The excess ROS generation will excite expression of heme oxygenase-1 and suppress CDA expression. Under low CDA expression, the inactivation of GEM is decreased in turn to exert excellent therapeutic efficiency. Herein, we first studied the ROS generation by DHA in vitro with A2780 cells by means of flow cytometry and confocal laser scanning microscopy. Furthermore, cytotoxicity assay in vitro showed that DHA + GEM had synergistic effect, with molar ratio of DHA and GEM at 10. Eventually, in A2780 ovarian cancer xenograft tumor model, DHA + GEM exhibited significant antitumor efficiency with lower blood toxicity than GEM alone. Noteworthy, the combination treatment group completely eliminated the tumors on day 14.

KEYWORDS

dihydroartemisinin, gemcitabine, ovarian cancer, reactive oxygen species

1 | INTRODUCTION

Human ovarian carcinoma is the leading cause of death from gynecological malignancy and the fifth among common cancer death.^{1,2} Most women with ovarian carcinoma were diagnosed at advanced stages and the 5-year survival for the patients has remained unchanged (<20%) over the past 20 years. It is still a challenge for the treatment of ovarian carcinoma.

Gemcitabine ([GEM]; 2',2'-difluorodeoxycytidine [dFdC]) is commonly used in chemotherapy for ovarian cancer, non-small-cell lung cancer, breast cancer, and pancreatic cancer.³⁻⁵ GEM is a prodrug, after entering the

cells, it can be phosphorylated stepwise by deoxycytidine kinase (dCK) into active 2',2'-difluorodeoxycytidine triphosphate (dFdCTP) metabolite.⁶⁻⁸ However, GEM is a pyrimidine nucleoside analogue of deoxycytidine and can be catalyzed to 2'-deoxy-2',2'-difluorouridine (dFdU), an inactive metabolite of GEM, by stromal and CDA.^{9,10} Indeed, it is reported that more than 90% GEM is inactivated into dFdU before dFdCTP incorporated into DNA strands to inhibit DNA replication and promote apoptosis in cancer cells.¹⁰ Therefore, the interference of CDA expression in cancer cells could decrease GEM inactivation, leading to increased drug uptake at the tumor site.

Artemisiae annuae Herba was initially used for treating fevers and then renowned to be an antimalarial herb,^{11,12} in which the most important active ingredient is artemisinin. Artemisinin was discovered and developed by Tu Youyou, for which she was awarded the 2015 Nobel Prize in Physiology or Medicine. Recent studies indicated that artemisinin showed high potential antitumor properties.¹³ Dihydroartemisinin (DHA) is one of important derivatives of artemisinin and also exhibits potent antimalarial ability and antitumor potential.¹⁴⁻¹⁷ Artemisinin and DHA possess an unusual intramolecular endoperoxide bridge and the endoperoxide bond can be activated by heme or ferrous iron to produce the cytotoxic reactive oxygen species (ROS).¹⁸⁻²¹ DHA can induce cancer cell apoptosis by producing excess ROS to cause oxidative damage to proteins, DNA, or lipids.²²⁻²⁴ It was reported that the higher oxidative stress could induce excess expression of heme oxygenase-1 (HO-1), which could further suppress cytidine deaminase (CDA) expression in cancer cells.^{25,26}

Herein, we report the synergistic effect of DHA + GEM on antitumor efficiency. We hypothesized that DHA could induce excess ROS generation, then the higher oxidative stress could induce excess expression of HO-1, which could suppress CDA expression and decrease the GEM inactivation in turn. Specifically, we take advantage of the DHA + GEM combination for the treatment of ovarian carcinoma A2780. The ROS generation by DHA was monitored by flow cytometry and confocal laser scanning microscopy (CLSM), meanwhile the cytotoxicity assay of DHA was conducted in vitro. In addition, the synergistic effect of DHA + GEM was verified in vitro and in vivo.

2 | MATERIALS AND METHODS

2.1 | Materials

DHA (Energy chemical, Shanghai, China), Cremophor EL (Aladdin, Shanghai, China), *N*-acetyl cysteine (NAC; Aladdin, Shanghai, China), 2',7'-dichlorodihydrofluorescein diacetate (DCF-DA; Aladdin, Shanghai, China), gemcitabine hydrochloride (GEM; Yangzhou Huihong Chemical Co. Ltd., Yangzhou, China) and 3-(4,5-dimethyl-thiazol-2-yl)-2,5-diphenyl tetrazolium bromide (MTT; Sigma-Aldrich, Shanghai, China), and Hoechst 33258 (Sigma-Aldrich, Shanghai, China) were used as received without further purification. All the other reagents were purchased from the Sinopharm Chemical Reagent Co. Ltd (Beijing, China) and used as received.

2.2 | Cell culture

Human ovarian cancer cell lines (A2780) and murine fibroblast cell lines (L929) were purchased from Shanghai

Bogoo Biotechnology Co. Ltd (Shanghai, China). The cells were cultured in Dulbecco modified Eagle medium (DMEM; Gibco, Grand Island, NY) with high glucose containing 10% fetal bovine serum (FBS), supplemented with 1% penicillin and 1% streptomycin incubating at 37°C in a 5% CO₂ atmosphere.

2.3 | Measurement of ROS generation

The generation of ROS induced by DHA was monitored by flow cytometry and CLSM with an oxidation-sensitive probe 2',7'-dichlorodihydrofluorescein diacetate (DCF-DA). The DCF-DA can be cleaved by nonspecific esterases and becomes highly fluorescent DCF upon oxidation by ROS.

For the flow cytometry assay, 4×10^5 A2780 or L929 cells per well were seeded in the six-well plates and incubated overnight with 2 mL DMEM, and then replaced with fresh DMEM containing DHA with or without NAC (10 mM). After 24 hours, the cells were washed with 3 mL phosphate-buffered saline (PBS) for three times, and incubated with DMEM containing DCF-DA (5 μM) for 1 hour at 37°C. Then the cells were washed with PBS for three times and treated by trypsin without EDTA and collected in 1 mL PBS. The cell suspension was centrifuged at 500g for 5 minutes and washed twice with 1 mL PBS. Eventually, the cells were suspended in 0.3 mL PBS for flow cytometry tests (BD Biosciences, San Jose, CA).

For the CLSM assay, 4×10^5 A2780 cells per well were seeded onto glass coverslips placed in the six-well plates and incubated overnight for cell adherence culture, then replaced with fresh DMEM with (a) DHA (50 μM), (b) DHA (100 μM), (c) DHA (100 μM) + NAC (10 mM), or (d) DHA (100 μM) + FeSO₄ (10 mM). After 24 hours, the cells were washed with 3 mL PBS for three times and incubated with DMEM containing DCF-DA (100 μM) for 1 hour at 37°C. Then the cells were washed with PBS for three times and fixed with 4% formaldehyde for 20 minutes at room temperature, followed by washing the residual formaldehyde with PBS for three times. According to the manufacturer's instructions, the cell nuclei were stained with Hoechst 33258. The coverslips were placed onto glass microscope slides and fixed with nail polish, and the fluorescence of DCF was visualized using a CLSM (Carl Zeiss LSM 700, Carl Zeiss, Jena, Germany).

2.4 | DHA cellular cytotoxicity assay in vitro

To verify the DHA could induce the cellular cytotoxicity by generating ROS, the A2780 cells were seeded in the 96-well plates with a density of 7000 cells per well and incubated overnight with 100 μL DMEM for cell adherence culture, then replaced with 200 μL fresh

DMEM with different concentration of DHA or DHA + NAC. The cells were subjected to MTT assay after being incubated for another 48 hours. Specifically, at the end of the experiments, 20 μ L MTT (1 mg/mL in sterile PBS) was added into the 96-well plates with 180 μ L fresh DMEM for another 4 hours incubation. The supernatant was removed and 100 μ L DMSO was added. The absorbance of the solution was measured on a Bio-Rad 680 microplate reader (Bio-Rad, Hercules, CA) at 490 nm. The relative cell viability (%) was calculated by the following formula:

$$\text{Cell viability (\%)} = (A_{\text{experimental}} / A_{\text{control}}) \times 100,$$

where $A_{\text{experimental}}$ and A_{control} represent absorbance of the experimental well and control well, respectively. Data are presented as average \pm SD ($n = 3$).

Similarly, the cellular cytotoxicity of DHA, FeSO₄ or their combination were also validated by MTT assay. The A2780 cells were seeded in the 12-well plates with a density of 10⁵ cells per well and incubated overnight with 100 μ L DMEM for cell adherence culture, then replaced with 1 mL fresh DMEM with different concentration of DHA or DHA + FeSO₄. The cells were subjected to MTT assay after being incubated for another 24 hours. Specifically, at the end of the experiments, 100 μ L MTT (1 mg/mL in sterile PBS) was added into the 12-well plates for another 4 hours incubation. The supernatant was removed and 500 μ L DMSO was added to test.

2.5 | The effect of DHA on HO-1 expression

To investigate the effect of DHA on HO-1 expression, Western blot analysis was carried out with whole-cell lysates. A2780 cells were treated with PBS or 50 μ M DHA for 24 hours. Whole-cell proteins were prepared by lysing the cells in RIPA Lysis Buffer supplemented with 1 mM proteinase inhibitor phenylmethanesulfonyl fluoride (PMSF) (Beyotime, Shanghai, China). After protein lysates were quantified, 40 μ g of protein was loaded into 15% polyacrylamide sodium dodecyl sulfate-polyacrylamide gel electrophoresis (SDS-PAGE) and electrophoretically transferred to polyvinylidene difluoride (PVDF) membranes (Bio-Rad). The membrane was blocked with Tris-buffered saline plus 0.1% Tween 20 plus 5.0% skim milk. Then PVDF membrane was incubated overnight with primary antibody against HO-1 (R&D Systems, Minneapolis, MN) at 4°C. Glyceraldehyde 3-phosphate dehydrogenase was used as an internal reference. The membrane was then washed and incubated for 1 hour with a secondary antibody. The proteins were visualized using an enhanced chemiluminescence Western blot

detection system (Tanon Science & Technology Co. Ltd., Shanghai, China).

2.6 | The effect of DHA on CDA expression

To investigate the influence of DHA on CDA expression, the immunocytochemistry (ICC) assay was conducted on A2780. The cells were seeded onto glass coverslips placed in the six-well plates with a density of 1.5×10^5 cells per well and incubated overnight for cell adherence culture, following treated with PBS or 50 μ M DHA for 24 hours. The cells were fixed with 4% formaldehyde (20 minutes) and permeated with 0.1% Triton X-100 (30 minutes). And then the cells were incubated with 5% bovine serum albumin for 1 hour to block nonspecific protein-protein interactions. The cells were incubated with the primary antibody against CDA (Abcam, Cambridge, MA) overnight at 4°C. The secondary antibody was fluorescein-5-isothiocyanate (FITC) conjugated goat anti-rabbit immunoglobulin G (IgG) (H + L) (ABclonal, Wuhan, China) used at a 1/50 dilution for 2 hours. Hoechst 33258 was used to stain the cell nuclei. The coverslips were placed onto glass microscope slides and fixed with nail polish, and visualized using a CLSM system.

2.7 | The synergistic effect of DHA and GEM in vitro

To investigate the interaction with GEM, the in vitro cytotoxicities of DHA and GEM on A2780 were assessed by MTT and apoptosis assay.

For the MTT assay, A2780 cells were seeded in 96-well plates at 5000 cells per well and incubated overnight with 100 μ L DMEM for cell adherence culture, then replaced with 200 μ L fresh DMEM with different concentration of DHA, GEM, or their combination. All the other procedures are similar to the above. The inhibitory concentration (IC_x) values are determined using Origin 9.2 according to the fitted data. The combination index (CI) was measured according to the Chou and Talalay's method.²⁷ To distinguish synergistic, additive, or antagonistic cytotoxic effects, the following equation was used:

$$CI_x = (D)_a / (D_x)_a + (D)_b / (D_x)_b,$$

where (D_x)_a and (D_x)_b represent the IC_x value of drug 'a' alone and drug 'b' alone, respectively. (D)_a and (D)_b represent the concentration of drug 'a' and drug 'b' in the combination system at the IC_x value. CI > 1 represents antagonism, CI = 1 represents additive, and CI < 1 represents synergism. In this study, IC₅₀

(inhibitory concentration to produce 50% cell death) was applied.

Cell apoptosis detection was performed by flow cytometry (FCM) analysis using annexin V-FITC apoptosis detection kit (KeyGEN Biotech, Nanjing, China). Approximately 4×10^5 A2780 cells were seeded in six-well plates and treated with DHA, GEM, or their combination at specific concentrations for 48 hours before analysis. The floating and trypsinized adherent cells were collected and prepared for detection according to the manufacturer's instructions. Samples were analyzed with a FACS Aria flow cytometer (BD Biosciences).

2.8 | Animals

Female Balb/C nude mice (6–8 weeks old) were obtained from Beijing Vital River Laboratory Animal Technology Co., Ltd. (Beijing, China). The mice were raised in specific pathogen-free animal laboratory. All animals received care in compliance with the guidelines outlined in the Guide for the Care and Use of Laboratory Animals and all procedures were approved by the Animal Care and Use Committee of Jilin University.

2.9 | Antitumor efficiency in vivo

A2780 cells (5×10^6 per mouse) were subcutaneously injected into the right flank to obtain ovarian cancer xenograft tumor model. The mice were divided into four groups randomly when the tumors volume reached approximately 120 mm^3 . The four groups mice were treated with PBS (control), DHA (95 mg/kg), GEM (10 mg/kg), or DHA + GEM (DHA 95 mg/kg, GEM 10 mg/kg) and injected on days 0, 3, 6, and 9. DHA was dissolved in Cremophor EL:ethanol:saline (1:1:8, vol/vol/vol) and administered via intraperitoneal (ip) injections. GEM was dissolved in PBS and administered intravenously via the tail vein (i.v.). The antitumor activity was evaluated by the tumor volumes (V_t), which were calculated using the following equations. Meanwhile, the body weight was measured simultaneously each other day as a symbol of the systemic toxicity. At the end of the assay, mice were killed. The tumors and major organs (heart, liver, spleen, lung, and kidney) were excised for histopathology analyses:

$$\text{Tumor volumes } (V_t, \text{ mm}^3) = a \times b^2/2,$$

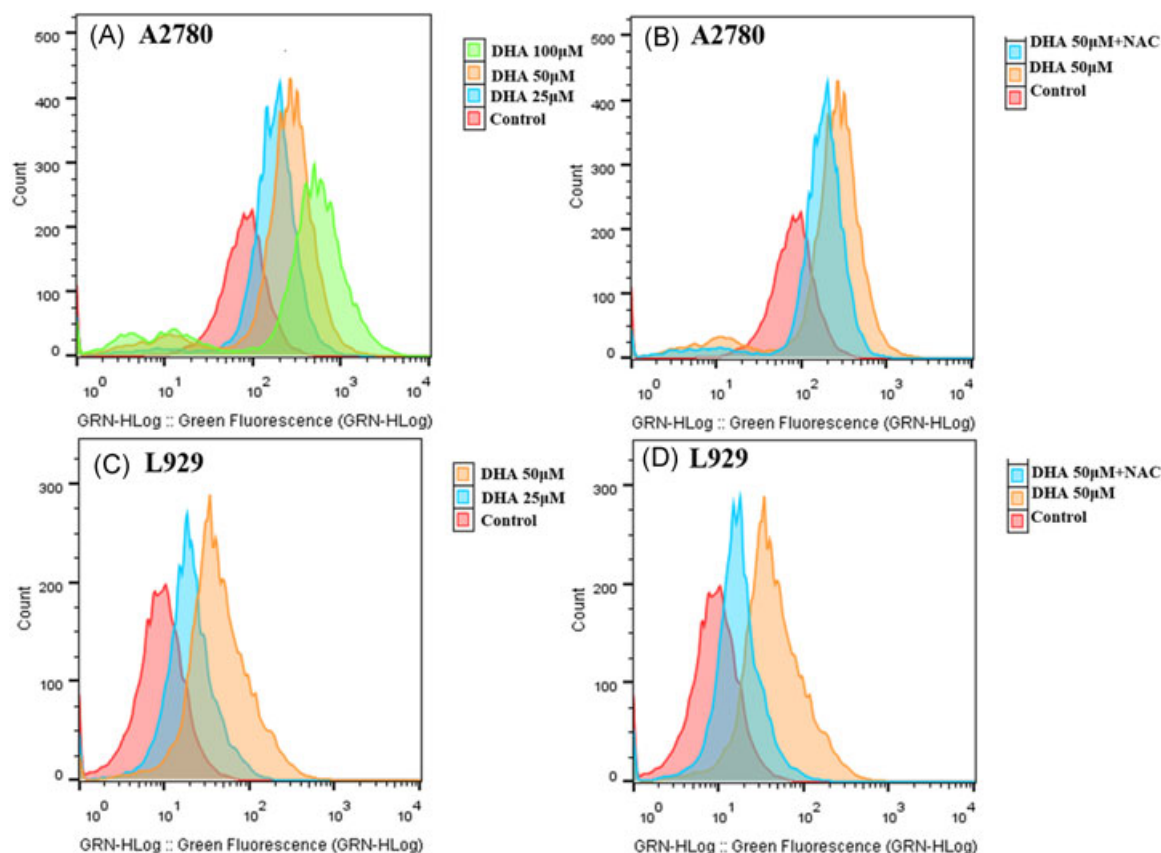


FIGURE 1 Flow cytometric images of DHA-induced ROS generation in A2780 and L929 cells with different DHA-treated concentration (A,C) and the production of ROS was markedly inhibited by pretreating the cells with NAC (B,D). DHA, dihydroartemisinin; NAC, *N*-acetyl cysteine; ROS, reactive oxygen species

where a and b represented the longest and shortest diameter of the tumors measured by a vernier caliper, respectively.

2.10 | Blood biochemistry and blood routine examination

Whole blood was collected from healthy nude mice after four repeated treatments at day 14. Blood was collected in a sodium EDTA anticoagulant tube for the hematology study. Red blood cells (RBC), white blood cells (WBC), platelets (PLT), hemoglobin (HGB), and hematocrits (HCT) were counted for the detection of myelosuppression.

2.11 | Histological and immunohistochemical analyses

The excised tumors and major organs were fixed in 4% PBS buffered paraformaldehyde overnight, and then embedded in paraffin. The paraffin-embedded tumors

and organs were cut at 5 μm thickness, and stained with hematoxylin and eosin (H&E) to assess histological alterations by optical microscope (Nikon TE2000U).

2.12 | Statistical analysis

All experiments were performed at least three times and expressed as means \pm SD. Data were analyzed for statistical significance using the Student t test. $P < 0.01$ was considered extremely significant difference.

3 | RESULTS

3.1 | The measurement of ROS generation

The ROS were analyzed using nonfluorescent DCF-DA, which could be activated into a green fluorescent product, DCF. The green fluorescent was measured by flow cytometer. As shown in Figure 1A, ROS was generated within A2780 cells treated with 25 μM DHA

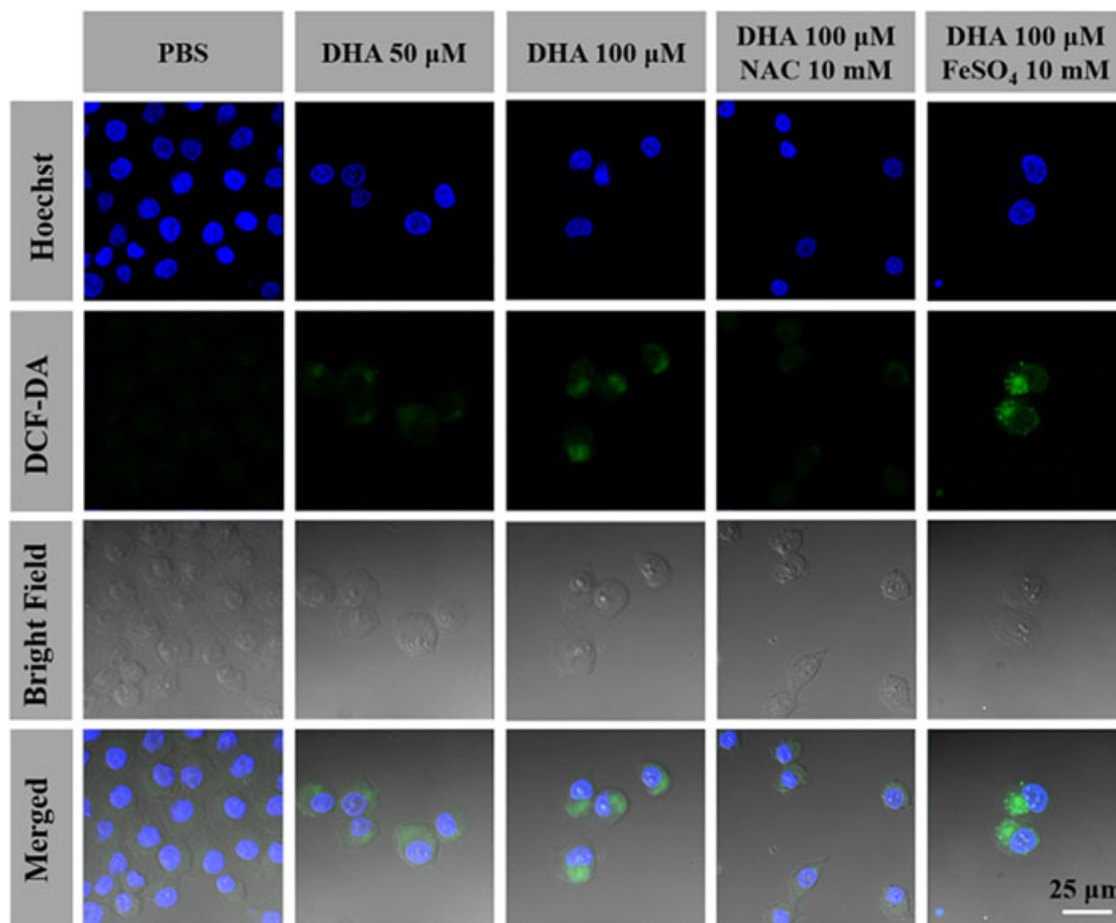


FIGURE 2 CLSM image of DHA-induced ROS generation in A2780 cells treated with PBS, DHA, or DHA + NAC, or DHA + FeSO_4 for 24 hours. Scale bar = 25 μm . CLSM, confocal laser scanning microscopy; DHA, dihydroartemisinin; NAC, *N*-acetyl cysteine; ROS, reactive oxygen species

and the green fluorescent was greatly enhanced with the increase of treated DHA concentration. It was thus concluded that DHA could induce ROS generation inside cells. Addition of *N*-acetyl cysteine (NAC), a ROS scavenger, could markedly decrease the green fluorescent (Figure 1B), proving the generation of ROS from another angle. Similar results were confirmed in fibroblast cell L929 (Figure 1C and 1D). Notably, the amount of inherent ROS generated in L929 was significantly lower compared with A2780 cancer cells, which indicates that the cancer cells were more vulnerable to the cytotoxic effects of DHA than normal cells.

Intracellular ROS generation was also detected by CLSM. As Figure 2 shows, the ROS was mainly produced in cytoplasm and ROS levels significantly increased in a concentration-dependent manner, which displayed consistent results from FCM analysis (Figure 1). The antioxidant NAC could abrogate the green DCF fluorescence, suggesting DHA treatment led to induction of ROS. The ROS generation by endoperoxide DHA was mediated by iron(II) heme. When adding additional ferrous ion (Fe(II)) (10 mM), the ROS generation was remarkably elevated, indicating that intramolecular endoperoxide bridge of DHA could be activated by ferrous iron to produce the cytotoxic ROS.

3.2 | DHA cellular cytotoxicity assay in vitro

The antitumor activity of DHA were conducted in A2780 cells. MTT assay manifested that DHA possessed a dose-dependent anticancer capability in A2780 cell lines. The DHA could induce cytotoxicity by generating ROS. Figure 3A showed that the NAC significantly attenuated cytotoxicity, which was in accordance with the decreased

ROS generation (Figure 1 and 2). DHA is a sesquiterpene lactone with an endoperoxide and DHA can be activated by ferrous iron to produce ROS via endoperoxide cleavage.²⁸ Moreover, the obvious cytotoxicity was observed when such extra ferrous ion was added into DHA (Figure 3B), indicating that DHA-reduced intracellular ROS were essential for DHA to exert its cytotoxic activity.

3.3 | The effect of DHA on HO-1 and CDA expression

DHA could induce intracellular ROS generation, simultaneously, HO-1, acted as a marker of oxidative stress, was performed by Western blot analysis. As shown in Figure 4A, DHA could significantly increase HO-1 expression on A2780 cells compared with PBS after 24 hours treatment. In addition, we evaluated the effect of DHA on CDA expression using ICC experiments. The green fluorescence intensity of DHA-treated cells was profoundly decreased (Figure 4B), indicating that DHA could downregulate the CDA expression.

3.4 | The synergistic effect of DHA and GEM in vitro

DHA could induce intracellular ROS generation to excite oxidative stress (HO-1 expression), which suppressed CDA expression. The lower expression of CDA in cells contributed to inhibit GEM metabolic inactivation. A series of different combination treatment ratios were conducted by MTT assay to investigate distinct interactions, ranging from antagonism to synergism. The IC₅₀ of the DHA and GEM on A2780 cells at 72 hours were 78.1 and 1.29 μ M, respectively. The combination index (CI) were calculated using the Chou and Talalay's method.

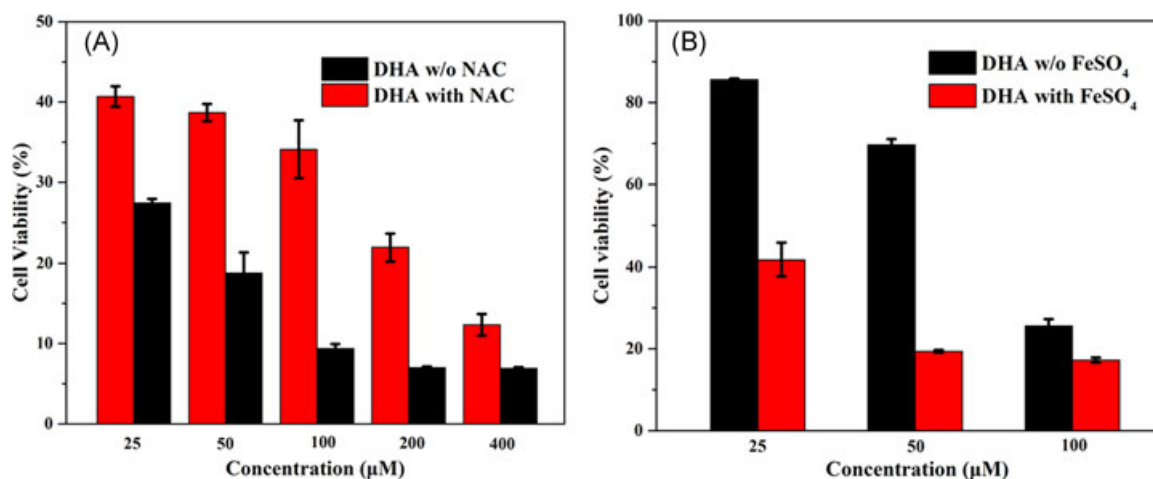


FIGURE 3 In vitro cell viabilities of A2780 cells incubated with DHA or DHA + NAC for 48 hours (A) and DHA or DHA + FeSO₄ for 24 hours (B). DHA, dihydroartemisinin; NAC, *N*-acetyl cysteine

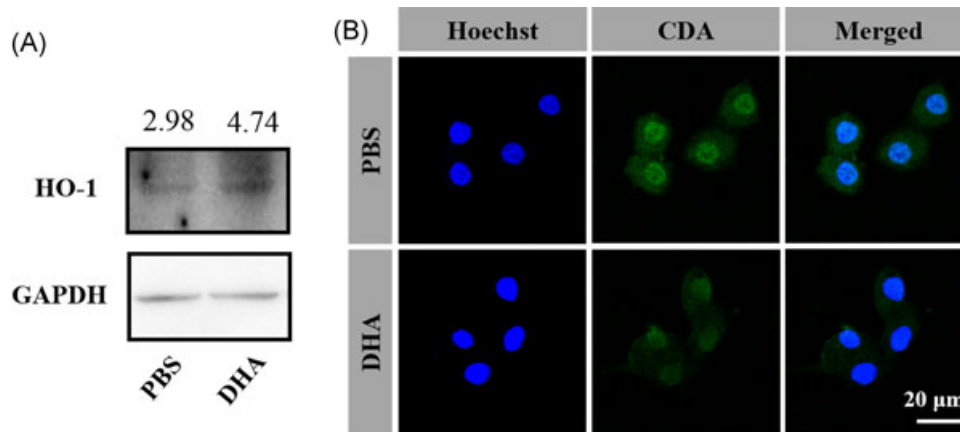


FIGURE 4 A, A2780 cells were treated with DHA for 24 hours, and then the protein samples were subjected to Western blot analysis. HO-1 expression was detected. B, CLSM image of A2780 cells after treated with DHA for 24 hours. The green fluorescence represented CDA expression. Scale bar = 20 μm . CLSM, confocal laser scanning microscopy; DHA, dihydroartemisinin; GAPDH, glyceraldehyde 3-phosphate dehydrogenase; HO-1, heme oxygenase-1; PBS, phosphate-buffered saline

The CI values of different combination treatment ratios were summarized in Table 1. When the molar ratio of DHA and GEM was 10, strong synergism was observed, with CI values 0.7, while the other ratio of the two drugs had suboptimal synergistic effect. Overall, employing the optimal molar ratio (DHA/GEM, 10:1, mol/mol) appeared to be necessary for maximal augmentation of antitumor activity in A2780 human ovarian cancer cells.

A2780 cells were treated with DHA, GEM, or their combination and cell apoptosis detection was conducted at 48 hours using annexin V-FITC apoptosis detection kit. The lower left quadrant (LL), upper left quadrant (UL), lower right quadrant (LR), and upper right quadrant (UR) represents live cells, fragments, and damage cells, early apoptosis, and late apoptosis cells, respectively. As shown in

TABLE 1 The IC_{50} of DHA, GEM, or their combination on A2780 cells at 72 h and the CI values of different DHA and GEM molar ratio

Entry	IC_{50} -DHA, μM	IC_{50} -GEM, μM	CI
DHA	78.10
GEM	...	1.29	...
DHA: GEM = 40:1	29.84	0.75	0.9
DHA: GEM = 20:1	16.74	0.84	0.8
DHA: GEM = 10:1	7.18	0.72	0.6
DHA:GEM = 1:1	1.67	1.67	1.3
DHA: GEM = 1:10	0.084	0.84	0.7

Abbreviation: CI, combination index; DHA, dihydroartemisinin; GEM, gemcitabine; IC, inhibitory concentration; NAC, *N*-acetyl cysteine; ROS, reactive oxygen species.

Figure 5, GEM could induce apoptotic rate for 39.6% and 25.7% of the cells in early apoptosis (LR) and in late apoptosis (UR), respectively. And the combination treatment group produced markedly more pronounced apoptosis than DHA or GEM alone treatment, the apoptotic of combination treatment were 54.5% (LR) and 37.0% (UR), respectively.

3.5 | Antitumor efficiency in vivo

Inspired by the pronounced antiproliferation effect of the DHA + GEM combination treatment in vitro, the antitumor efficiency of the DHA, GEM, or the DHA + GEM combination on A2780 ovarian cancer xenograft tumor model was conducted. When the tumors were about 120 mm^3 , mice received the treatment with PBS, DHA (ip), GEM (iv) or DHA + GEM combination on days 0, 3, 6, and 9. Tumor volumes and mice body weights were measured every other day. As Figure 6A shows, DHA-treated group had inconspicuous therapeutic effects compared with control group and mice treated with GEM showed remarkable inhibition on tumor growth. While the DHA + GEM combination treatment group had unexpected antitumor efficiency, the tumors were completely eliminated on day 14 (Figure 6B). The changes of mice body weight were a symbol of systemic toxicity. As shown in Figure 6C, the three treated groups had no weight descends, indicating that the DHA + GEM combination treatment was worth taking.

3.6 | Blood biochemistry and blood routine examination

Since the major side effect of GEM was myelosuppression, blood routine examination was conducted on day 14 (Figure 7). Owing to the lower treatment dose and

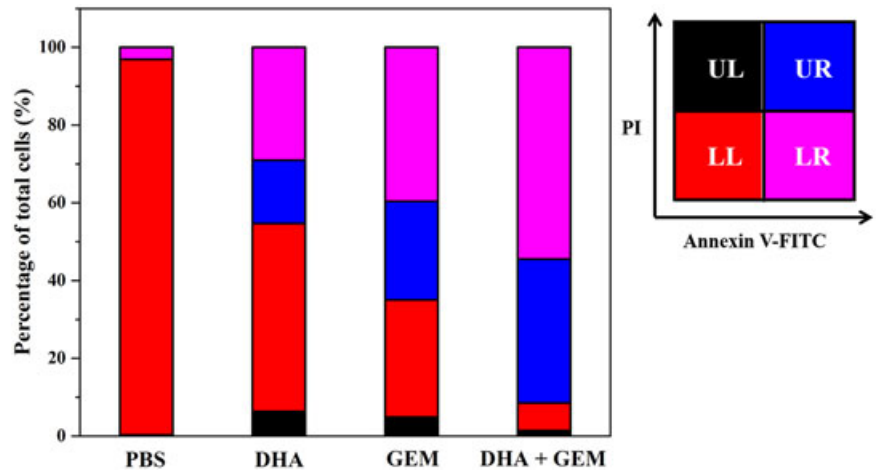


FIGURE 5 Cell apoptosis of A2780 cells treated with DHA, GEM, or the combination for 48 hours and measured by flow cytometry. DHA, dihydroartemisinin; GEM, gemcitabine

reasonable treatment time design of DHA + GEM, the levels of platelets (PLT), white blood cells (WBC), red blood cells (RBC), hemoglobin (HGB), and hematocrit (HCT) were close to the value of the untreated control. However, the GEM alone treatment group has slight increase in the levels of PLT and WBC on day 14, while the DHA + GEM treatment group had no noticeable aggravation of blood toxicity.

ability of tumor cell (Figure 8). The degrees of tumor tissue necrosis treated with DHA were unobvious, which was consistent with the antitumor efficiency. However, the overt tumor tissue necrosis was observed when mice were treated with GEM. In addition, there was no obvious necrosis or significant morphological changes of heart, liver, spleen, lung, and kidney derived from mice in treatment groups compared to control group.

3.7 | Histological and immunohistochemical analyses

The tumors and major organs were collected at the end of the antitumor experiments. Through histological analysis using H&E staining to tissue slices, the therapeutic effects of the DHA, GEM or DHA + GEM combination were assessed. Owing to the complete elimination of tumors of the DHA + GEM combination group, there was no representative H&E picture of the tumor. For the H&E staining, the tumor treated with PBS had large nuclei and more chromatin, revealing the powerful proliferation

4 | DISCUSSION

Compared with normal cells, cancer cells have higher levels of ROS and oxidative stress.²⁹ And ROS could influence and regulate the expression of proteins in signal transduction pathways.³⁰ Therefore, regulating the level of ROS by adding some redox reagents is a way to adjust protein expressions. It is reported that the higher oxidative stress could induce excess expression of HO-1. In the current study, we take advantage of DHA to produce excess of ROS in cancer cells. DHA possesses an endoperoxide bridge

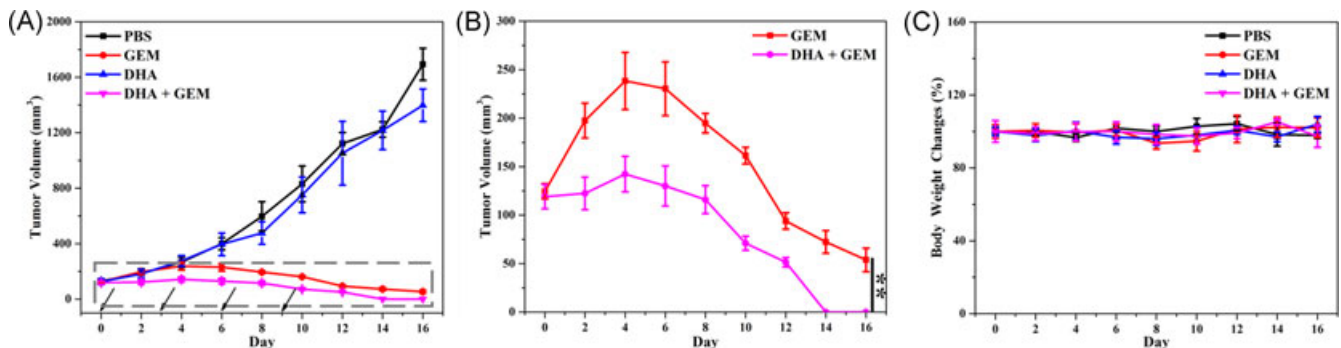


FIGURE 6 In vivo antitumor efficacy of PBS (control), DHA (95 mg/kg), GEM (10 mg/kg), or the combination therapy of DHA + GEM (DHA, 95 mg/kg and GEM, 10 mg/kg) and injected on days 0, 3, 6, and 9 in A2780 tumor-bearing Balb/C nude mice. A, Tumor volume increment during the treatment. The black arrows represent the treatment day. B, The amplification of the GEM and combination therapy antitumor curves. C, Body weight changes of A2780 tumor-bearing mice during the treatment. The data are shown as mean ± SD (n = 5). **P < 0.01. DHA, dihydroartemisinin; GEM, gemcitabine; PBS, phosphate-buffered saline

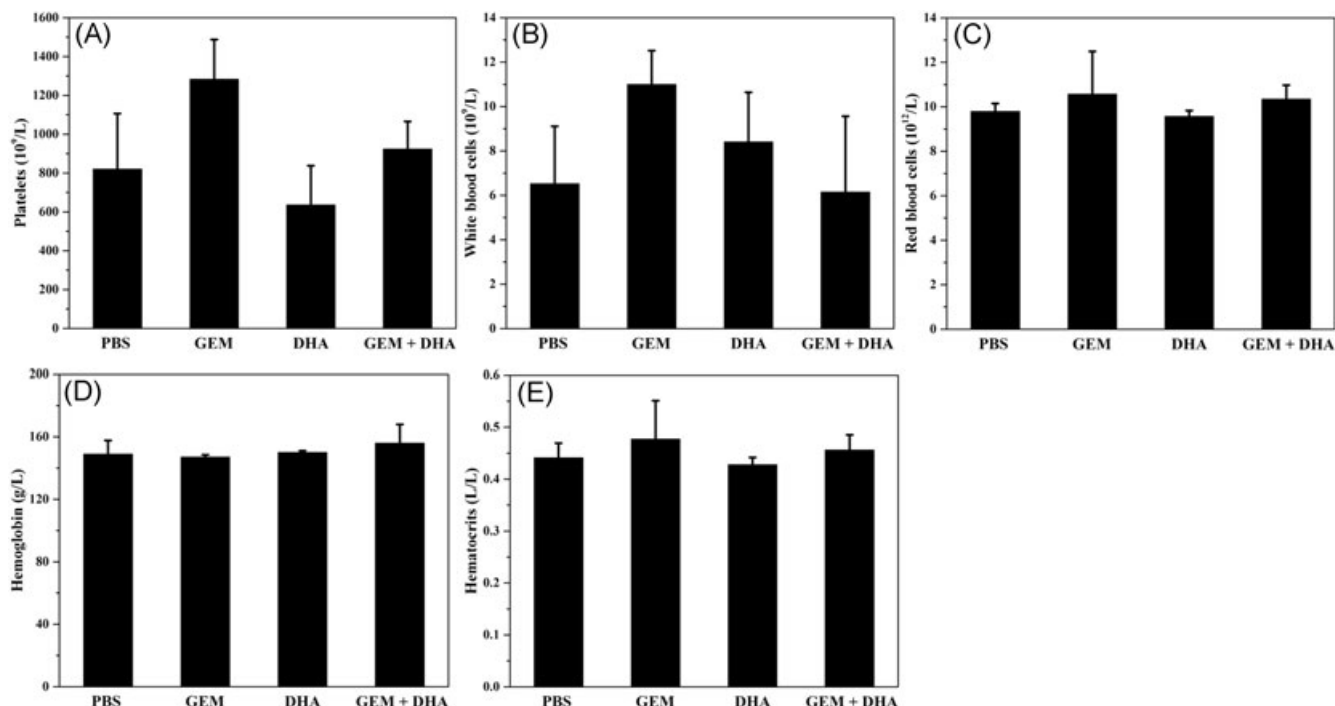


FIGURE 7 The hematological parameters of the mice after treatment with PBS, DHA, GEM, or DHA + GEM for 14 days. DHA, dihydroartemisinin; GEM, gemcitabine; PBS, phosphate-buffered saline

structure and the endoperoxide bridge could be broken with free ferrous iron and heme as activators.^{31,32} The broken endoperoxide bridge of DHA generates oxygen radicals and further increases ROS in cells. We have demonstrated that DHA could increase ROS levels in vitro and if adding extra ferrous iron, the ROS generation was remarkably elevated, indicating that intramolecular endoperoxide bridge of DHA

could be activated by ferrous iron to produce the cytotoxic ROS.

In this contribution, we utilized DHA to suppress CDA expression. Specifically, DHA could elevate the ROS levels and HO-1, a marker of oxidative stress, is increased simultaneously.³³ Increased HO-1 would finally suppress the expression of CDA. In comparison, a ROS scavenger

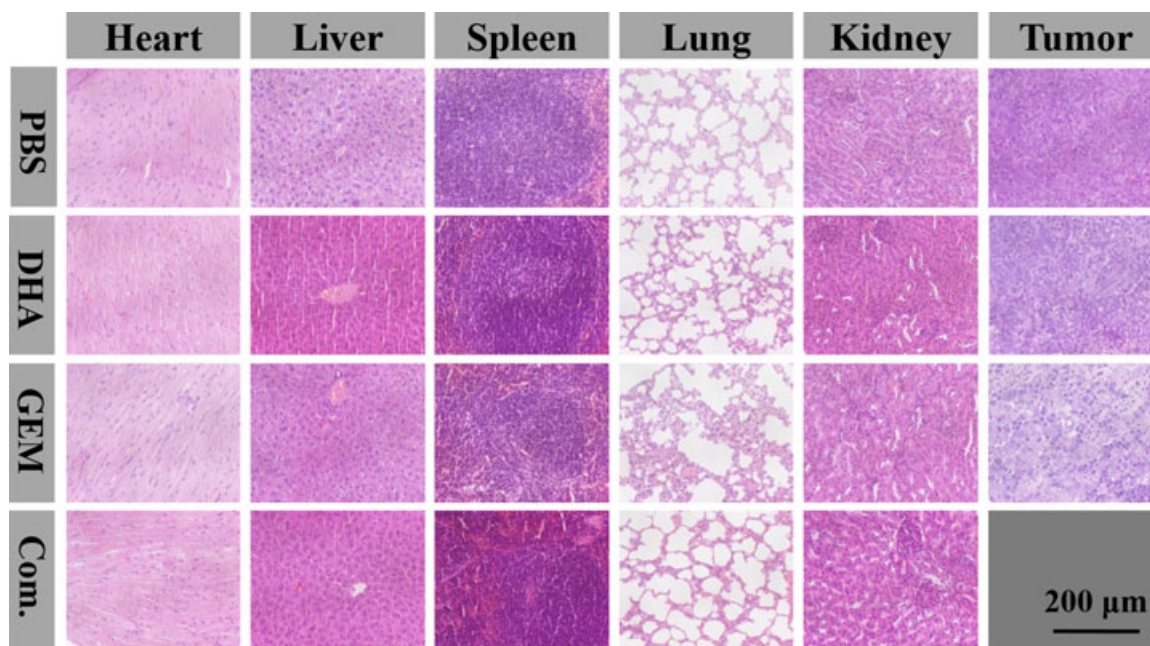


FIGURE 8 Histologic assessments of major organs and tumors with H&E staining in A2780 tumor-bearing Balb/C nude mice. Scale bar = 200 μ m. H&E, hematoxylin and eosin

NAC could markedly decrease the ROS level in vitro. As revealed by Frese et al,²⁵ NAC could inhibit HO-1 expression. GEM is a pyrimidine nucleoside analogue of deoxycytidine and could be catalyzed by stromal and cellular CDA to dFdU, an inactive metabolite of GEM.¹⁰ The decreased CDA expression contributed to the lower production of dFdU. Hence, a series of different combination treatment ratios of DHA and GEM were conducted by MTT assay to investigate distinct interactions, ranging from antagonism to synergism. When the molar ratio of DHA and GEM were 10, strong synergism was observed, with CI values 0.7.

Ovarian carcinoma is the leading cause of death from gynecological malignancy.² A2780, a human ovarian cancer cell lines, were subcutaneously injected into the right flank of Balb/C nude mice to obtain ovarian cancer xenograft tumor model. The DHA + GEM combination treatment group had unexpected antitumor efficiency, the tumors were completely eliminated on day 14.

In summary, we had demonstrated that the DHA could produce cellular ROS generation and the excess ROS could induce cell apoptosis. The obvious cytotoxicity was observed when such extra ferrous ion was added into DHA. The synergistic effect of DHA + GEM in vitro were verified in A2780 cells and we also obtained the optimal molar ratio (DHA/GEM, 10:1, mol/mol). Moreover, the combination treatment group produced markedly more pronounced apoptosis than treatment under DHA or GEM alone. In vivo antitumor efficacy of ovarian cancer A2780, DHA + GEM combination treatment group exhibited excellent antitumor activity and lower systemic toxicity than GEM alone. Noteworthy, the combination treatment group completely eliminated the tumors on day 14.

ACKNOWLEDGMENTS

This study was financially supported by Ministry of Science and Technology of China (Projects 2016YFC1100701 and 2017zx09101005-012), National Natural Science Foundation of China (Projects 51673189, 51528303, 51503202, 51520105004, and 51390484), Science and Technology Service Network Initiative (Project KFJ-SW-STS-166), and the Chinese Academy of Sciences Youth Innovation Promotion Association.

CONFLICTS OF INTEREST

The authors declare no conflict of interest.

ORCID

Zhaohui Tang  <http://orcid.org/0000-0003-4726-4305>

REFERENCES

- Greenshields AL, Shepherd TG, Hoskin DW. Contribution of reactive oxygen species to ovarian cancer cell growth arrest and killing by the anti-malarial drug artesunate. *Mol Carcinog.* 2017;56:75-93.
- Dia VP, Pangloli P. Epithelial-to-mesenchymal transition in paclitaxel-resistant ovarian cancer cells is downregulated by luteolin. *J Cell Physiol.* 2017;232:391-401.
- Bildstein L, Dubernet C, Marsaud V, et al. Transmembrane diffusion of gemcitabine by a nanoparticulate squalenoyl prodrug: an original drug delivery pathway. *J Control Release.* 2010;147:163-170.
- Zhang L, Wu C, Zhang Y, et al. Efficacy comparison of traditional Chinese medicine LQ versus gemcitabine in a mouse model of pancreatic cancer. *J Cell Biochem.* 2013;114:2131-2137.
- Chen G, Svirskis D, Wen J. Development and validation of a stability indicating isocratic HPLC method for gemcitabine with application to drug release from poly lactic-co-glycolic acid nanoparticles and enzymatic degradation studies. *J Pharm Pharmacol.* 2015;67:1528-1536.
- Galmarini CM, Clarke ML, Falette N, Puisieux A, Mackey JR, Dumontet C. Expression of a non-functional p53 affects the sensitivity of cancer cells to gemcitabine. *Int J Cancer.* 2002;97:439-445.
- Moysan E, Bastiat G, Benoit J-P. Gemcitabine versus modified gemcitabine: a review of several promising chemical modifications. *Mol Pharm.* 2013;10:430-444.
- Ohmine K, Kawaguchi K, Ohtsuki S, et al. Quantitative targeted proteomics of pancreatic cancer: deoxycytidine kinase protein level correlates to progression-free survival of patients receiving gemcitabine treatment. *Mol Pharm.* 2015;12:3282-3291.
- Pasut G, Canal F, Dalla Via L, Arpicco S, Veronese FM, Schiavon O. Antitumoral activity of PEG-gemcitabine prodrugs targeted by folic acid. *J Control Release.* 2008;127:239-248.
- Ye FG, Song CG, Cao ZG, et al. Cytidine deaminase axis modulated by miR-484 differentially regulates cell proliferation and chemoresistance in breast cancer. *Cancer Res.* 2015;75:1504-1515.
- Zhang ZS, Wang J, Shen YB, et al. Dihydroartemisinin increases temozolomide efficacy in glioma cells by inducing autophagy. *Oncol Lett.* 2015;10:379-383.
- Dai Y-F, Zhou W-W, Meng J, et al. The pharmacological activities and mechanisms of artemisinin and its derivatives: a systematic review. *Med Chem Res.* 2017;26:867-880.
- Xu CC, Deng T, Fan ML, Lv WB, Liu JH, Yu BY. Synthesis and in vitro antitumor evaluation of dihydroartemisinin-cinnamic acid ester derivatives. *Eur J Med Chem.* 2016;107:192-203.
- Kong R, Jia G, Cheng Z, et al. Dihydroartemisinin enhances Apo2L/TRAIL-mediated apoptosis in pancreatic cancer cells via ROS-mediated up-regulation of death receptor 5. *PLoS One.* 2012;7:e37222.
- Li Y, Wang Y, Kong R, et al. Dihydroartemisinin suppresses pancreatic cancer cells via a microRNA-mRNA regulatory network. *Oncotarget.* 2016;7:62460-62473.
- Zhang CZ, Zhang H, Yun J, Chen GG, Lai PBS. Dihydroartemisinin exhibits antitumor activity toward hepatocellular

- carcinoma in vitro and in vivo. *Biochem Pharmacol.* 2012;83:1278-1289.
17. Chen SS, Hu W, Wang Z, Lou XE, Zhou HJ. p8 attenuates the apoptosis induced by dihydroartemisinin in cancer cells through promoting autophagy. *Cancer Biol Ther.* 2015;16:770-779.
 18. Liu L, Wei Y, Zhai S, Chen Q, Xing D. Dihydroartemisinin and transferrin dual-dressed nano-graphene oxide for a pH-triggered chemotherapy. *Biomaterials.* 2015;62:35-46.
 19. Wang J, Zhang CJ, Chia WN, et al. Haem-activated promiscuous targeting of artemisinin in *Plasmodium falciparum*. *Nat Commun.* 2015;6:10111.
 20. Chaturvedi D, Goswami A, Pratim saikia P, Barua NC, Rao PG. Artemisinin and its derivatives: a novel class of anti-malarial and anti-cancer agents. *Chem Soc Rev.* 2010;39:435-454.
 21. Crielaard BJ, Lammers T, Rivella S. Targeting iron metabolism in drug discovery and delivery. *Nat Rev Drug Discov.* 2017;16:400-423.
 22. Gerhardt T, Jones R, Park J, et al. Effects of antioxidants and pro-oxidants on cytotoxicity of dihydroartemisinin to Molt-4 human leukemia cells. *Anticancer Res.* 2015;35:1867-1871.
 23. Wang Q, Wu S, Zhao X, Zhao C, Zhao H, Huo L. Mechanisms of dihydroartemisinin and dihydroartemisinin/holotransferrin cytotoxicity in T-cell lymphoma cells. *PLoS One.* 2015;10:e0137331.
 24. Zhang CJ, Wang J, Zhang J, et al. Mechanism-guided design and synthesis of a mitochondria-targeting artemisinin analogue with enhanced anticancer activity. *Angew Chem Int Ed Engl.* 2016;55:13770-13774.
 25. Frese KK, Neesse A, Cook N, et al. nab-Paclitaxel potentiates gemcitabine activity by reducing cytidine deaminase levels in a mouse model of pancreatic cancer. *Cancer Discov.* 2012;2:260-269.
 26. Meng H, Wang M, Liu H, et al. Use of a lipid-coated mesoporous silica nanoparticle platform for synergistic gemcitabine and paclitaxel delivery to human pancreatic cancer in mice. *ACS Nano.* 2015;9:3540-3557.
 27. Chou TC. Drug combination studies and their synergy quantification using the Chou-Talalay method. *Cancer Res.* 2010;70:440-446.
 28. van Agtmael MA, Eggelte TA, van Boxtel CJ. Artemisinin drugs in the treatment of malaria: from medicinal herb to registered medication. *Trends Pharmacol Sci.* 1999;20:199-205.
 29. Trachootham D, Alexandre J, Huang P. Targeting cancer cells by ROS-mediated mechanisms: a radical therapeutic approach. *Nat Rev Drug Discov.* 2009;8:579-591.
 30. Valko M, Leibfritz D, Moncol J, Cronin MTD, Mazur M, Telser J. Free radicals and antioxidants in normal physiological functions and human disease. *Int J Biochem Cell Biol.* 2007;39:44-84.
 31. Bai J, Jia X, Zhen W, Cheng W, Jiang X. A facile ion-doping strategy to regulate tumor microenvironments for enhanced multimodal tumor theranostics. *J Am Chem Soc.* 2018;140:106-109.
 32. Efferth T, Benakis A, Romero MR, et al. Enhancement of cytotoxicity of artemisinins toward cancer cells by ferrous iron. *Free Radic Biol Med.* 2004;37:998-1009.
 33. Kim KA, Kook SH, Song JH, Lee JC. A phenolic acid phenethyl urea derivative protects against irradiation-induced osteoblast damage by modulating intracellular redox state. *J Cell Biochem.* 2014;115:1877-1887.

How to cite this article: Yang S, Zhang D, Shen N, Wang G, Tang Z, Chen X. Dihydroartemisinin increases gemcitabine therapeutic efficacy in ovarian cancer by inducing reactive oxygen species. *J Cell Biochem.* 2019;120:634-644.
<https://doi.org/10.1002/jcb.27421>